

Radiation belt dynamics and the decay time scale of electrons at different energy and altitude

Zhiyuan Guo^{1*}

¹The University of Illinois at Urbana Champaign, Champaign, Illinois, United States of America

* Corresponding author email: zg13@illinois.edu

Abstract. Since the discovery of the Radiation belt, scientists have had strong interests in the magnetized space that protects us from the bombardment of solar storms. Early satellite observations show that the radiation belts consist of energetic particles and exhibit a two-belt structure. The outer belt electrons are accelerated during geomagnetic storms, while the inner-belt is mostly formed by the cosmic ray. Recently, the NASA Van Allen probes discovered a temporary storage ring that locates in the middle of the two belts when solar storm event occurs, and the radiation belts may exhibit a three-belt structure. This study aims to analyze the three-belt structure from short-term variation and long-term variation. We calculated the decay time scale in the heart of the radiation belt which describes the lifetime of the high-energy electrons. The study of the decay time is of great significance in understanding the dynamics of the whole radiation belt.

Keywords: Van Allen Belt, geomagnetic storms, three belt structure, decay time scale.

1. Introduction.

1.1 Introduction to Radiation Belt.

Earth's Radiation Belt, also known as the Van Allen Belt, was discovered in 1958 by James A. Van Allen. The radiation belt locates between $1.2 < L$ (Earth Radii) < 7 in Earth's outer space [1]. The belt is formed by high-energy particles (electrons and protons) transported by the solar wind. When they reached the Earth's outer space, its magnetic field was strong enough to trap and convert them to outer space [2].

Before the launching of Van Allen Probe, the radiation belt was considered to have three parts: an outer belt and an inner belt. The outer belt is called the magnetosphere, and it is highly dynamic because of the direct interaction with the solar wind. The inner belt is formed by the interaction between Earth's atmosphere and cosmic rays [2]. The Figure 1 below shows a typical two-belt structure's cross-section view.

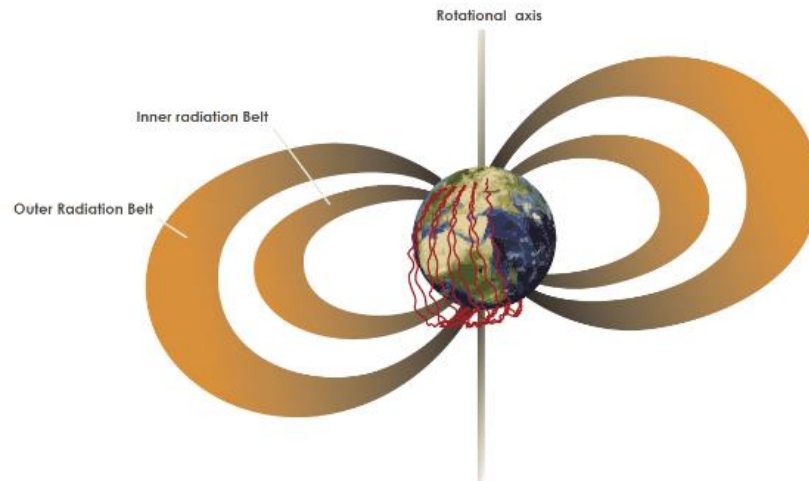


Figure 1. the cross-section view of a typical two-belt structure [3].

But after NASA launched the Van Allen Probe mission, the data gathered showed different views of the radiation belt.

1.2 Introduction to Van Allen Probes

Van Allen Probes, also known as the Radiation Belt Storm Probes, are two identical probes that rotate around the Earth in the same elliptical orbit, with one following the other. Their job is to answer the question of how the high energy made their way to the Earth and what have they done to the Earth's outer space [4]. They were launched on August 30, 2012, and still withstanding the intense radiation. The orbit lies near the Earth's equator and has a different altitude between 375 miles and 20,000 miles above Earth's surface [5].

The advantage of having two satellites in one system is that scientists can compare the two data sets and determine how the event occurs: simultaneously throughout the belts, at a single point in space, or jumping from one point to another.

The probe consists of multiple instruments: RBSPICE, RPS, EFW, EMFISIS, and ECT. With all the data collected by the instruments, scientists can understand how the Van Allen Radiation belt reacts with solar activities. The Figure 2 below shows one Van Allen probe and where the instruments are located [6].

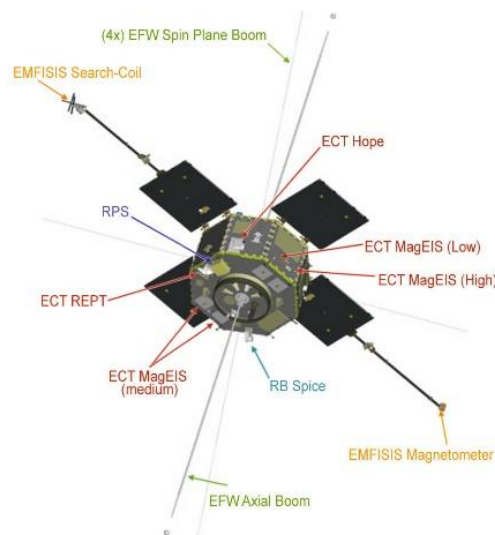


Fig 2. Van Allen probe with the instruments indicated [6].

1.3 Introduction to Geomagnetic Storms

Geomagnetic storms happen when the solar wind has strongly dynamic interactions, usually the exchange of energy, with Earth's outer space. These interactions are reflected as the disturbance of the magnetosphere. The interactions would cause fluctuations in the magnetosphere's currents, plasmas, and fields. High-speed solar wind that can last several or more hours is optimal for creating geomagnetic storms.

Solar coronal mass ejections are one of the banes under the largest storms. When the ejection occurs, a billion or more tons of plasma is thrown out of the Sun, then several days later, the plasma mass and its magnetic field will bombard the Earth's magnetosphere. High-speed solar wind stream is also responsible for some large storms. The stream intertwines with slower solar winds and circulates them, creating co-rotating interaction regions. Since the co-rotating interaction regions are not as fast as the coronal ejection, they will stay longer and exchange more energy with Earth's magnetosphere [7]. The Figure 3 below shows the result of the interactions that human eyes can see called the aurora [7].



Figure 3. One of the results of the geomagnetic storms, aurora [7].

1.4 Goal of this study.

Before the launching of the Van Allen probe, scientists agreed more on the two-belt structure model scholarly because the probes before never had enough resolution to specify the temporary third belt, called the relativistic electron storage ring, in the middle, which is created by the major solar wind events. This study aims to identify this third belt in short-term and long-term variations of the radiation belt dynamics and how the solar wind event can continue to affect the radiation belt. Then the final step is to calculate how long can the third belt last in one specific event through an energy level. The Figure 4 below shows the typical three-belt structure.

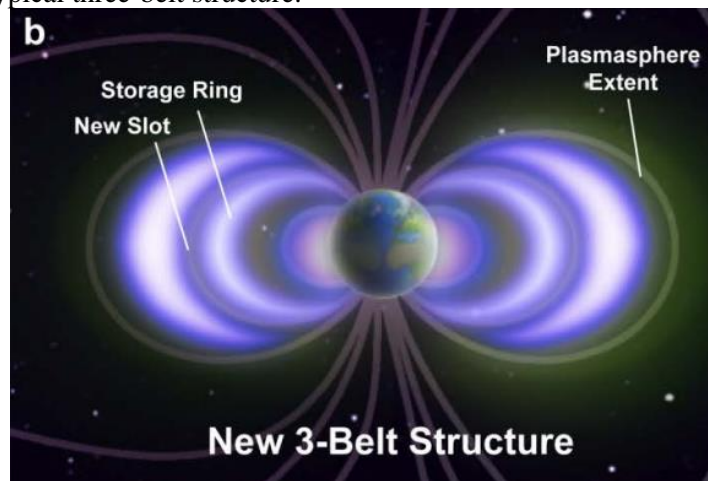


Figure 4. The typical three-belt structure with a Storage Ring between the magnetosphere and the inner belt [8].

2. Long-term and short-term variation of radiation belt dynamics.

Now in this section, we are going to take a closer look at the short-term variations and long-term variations of the radiation belt dynamics to determine how the solar wind magnitude, reflected as the Sym-H index (how strong is the Earth's magnetic field timewise), affects the electron flux index, which can be converted to the altitude of the high-energy electrons in terms of Earth Radii in different energy levels [9].

2.1 Short-term variations

For the short-term variation, we choose the time interval between March 13th 2013, and March 23rd 2013. The Figure 5 below shows the Sym-H index (unit nT) vs. date, electron flux (unit $s^{-1}cm^{-2}sr^{-1}MeV^{-1}$) vs. date, and the colored graph shows the relationship between the electron flux and the altitude (unit Earth Radii) in 1.8 MeV energy level. The color bar indicates the Flux range between 10 to 1010 $s^{-1}cm^{-2}sr^{-1}MeV^{-1}$.

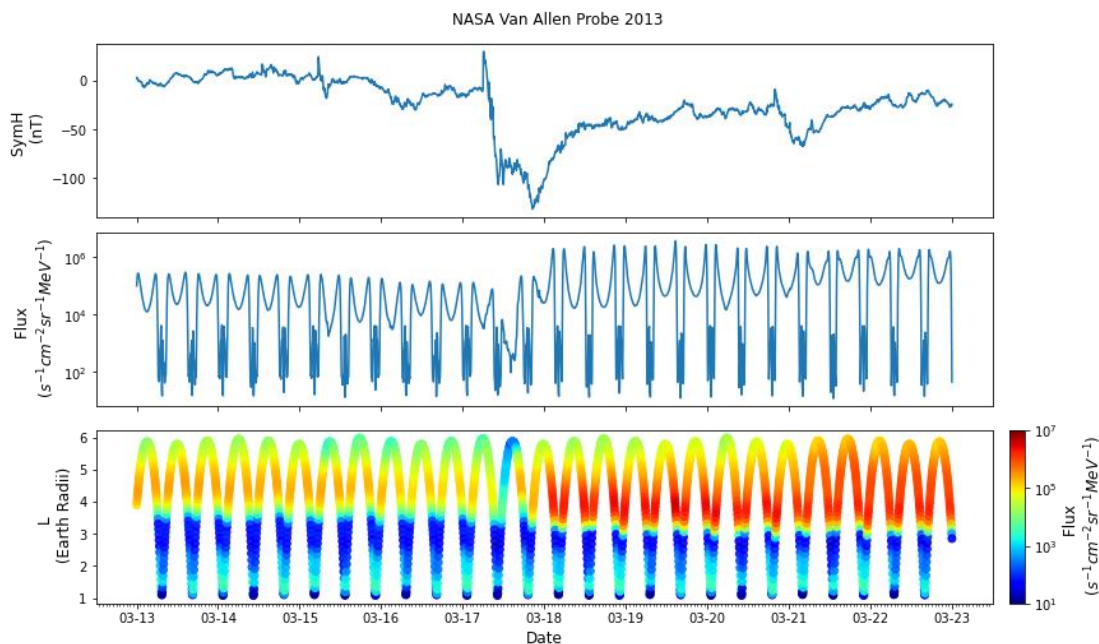


Figure 5. Short-term variation of the radiation belt between March 13th 2013, and March 23rd 2013.

From this graph, we can see that when the Sym-H index has a virulent fluctuation, the Flux will rise and then stably decrease for a while. The electron flux jumps from 103 to over 106. In the third graph, the high-energy electrons clustered and gained an enormous amount of energy after a short energy loss between March 17th and March 18th.

One advantage of studying short-term variations is knowing more detailed information about one specific event such as this one. Yet one disadvantage of short-term variation is that it's harder to analyze whether the event created a three-belt structure. Only looking at this graph, it seems that the radiation belt only has a two-belt structure, one outer belt from $L = 3$ to $L = 6$, and one inner belt from $L = 3$ to $L = 1$.

2.2 Long-term variations

For the long-term variation, we choose the whole of 2015 as the range and created a similar graph to the short-term variation graph. The energy levels from the third graph are 1.8 MeV with a flux range of 10 to 107 $s^{-1}cm^{-2}sr^{-1}MeV^{-1}$, 2.1 MeV with a flux range of 10 to 107 $s^{-1}cm^{-2}sr^{-1}MeV^{-1}$, 2.6 MeV with a flux range of 10 to 107 $s^{-1}cm^{-2}sr^{-1}MeV^{-1}$, 3.4 MeV with a flux range of 10 to 107 $s^{-1}cm^{-2}sr^{-1}MeV^{-1}$, 4.2 MeV with a flux range of 10 to 107 $s^{-1}cm^{-2}sr^{-1}MeV^{-1}$, 5.2 MeV with a flux range of 10 to 107 $s^{-1}cm^{-2}sr^{-1}MeV^{-1}$, and 6.3 MeV with a flux range of 10 to 107 $s^{-1}cm^{-2}sr^{-1}MeV^{-1}$.

The Figure 6 below clearly shows the major storm events across the year via Sym-H indices, and the electron flux is moving accordingly. When the Sym-H index drops, the electron flux rises and decreases just as we expected. For the energy levels 1.8 MeV and 2.1 MeV, it's not apparent to recognize the temporary three-belt structures, but the higher the energy level is, the clearer the storage belt is for each major storm event, such as the storm event in the middle of March 2015 and the events in June and July. The pattern of the storage belt is usually seen between $L = 3$ and $L = 2$, as the graph depicted.

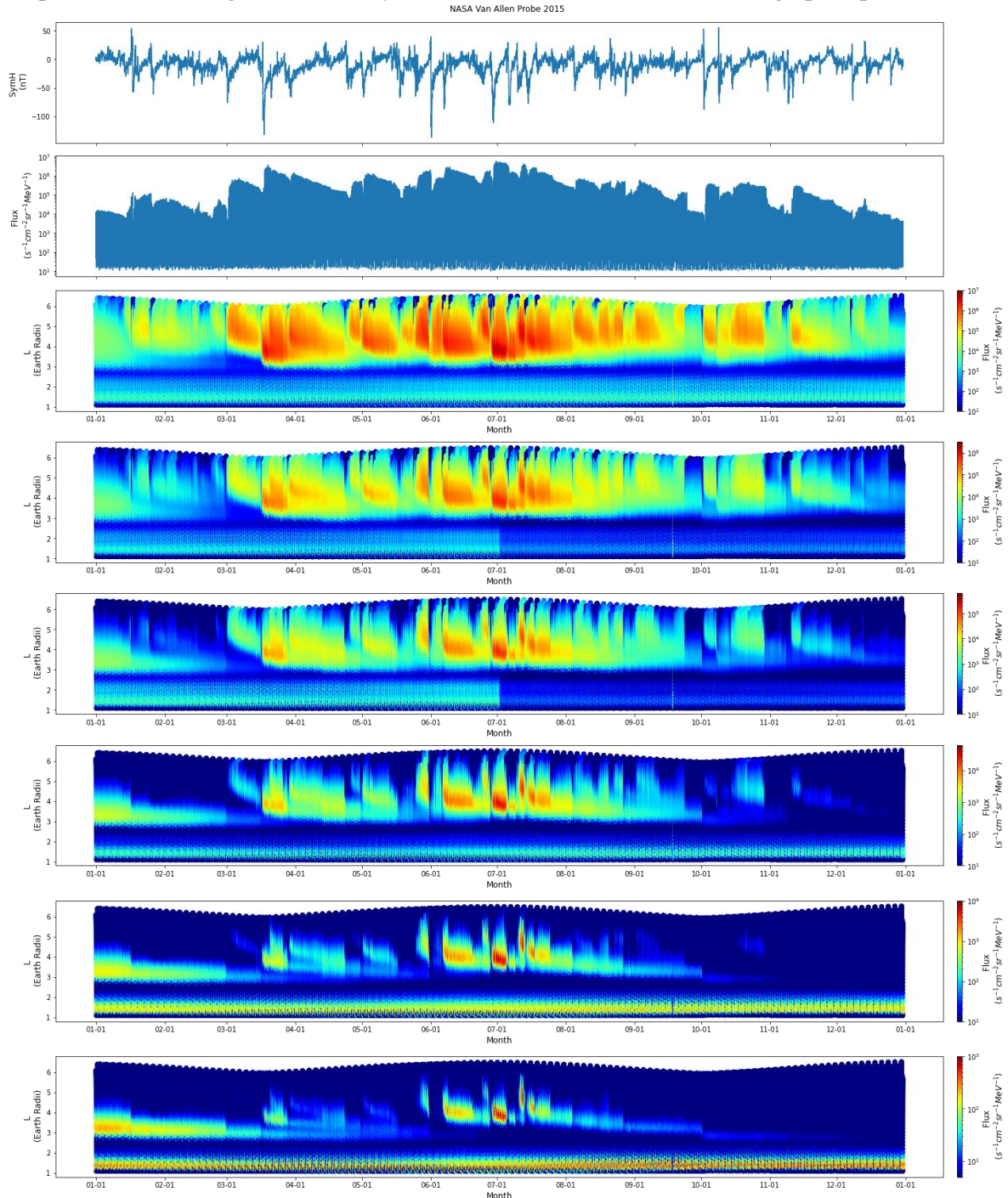


Figure 6. Long-term variation for the radiation belt dynamics for 2015 and different energy level electron flux coordinates.

2.3 Motion of electron flux and three-belt structure.

From both the short-term variation graph and the long-term variation graph, when the Sym-H index has a major fluctuation, the electron flux will respond favorably, which shows that the stronger the solar wind is, the more energy it would exchange with the magnetosphere. Although from short-term variation, it's hard to recognize the temporary three-belt structure, it is much more apparent in the long-term variation graph in.

3. Calculate the decay time scale of electrons at different energy and altitude (L value).

Next step, we will calculate the decay time scale, tau, of the relativistic electron storage ring by using the exponential fitting and show our results as the best-fitted regression line of the log Flux. Since the solar storm event can't last forever, the third belt is also temporary. For a specific event, we can gather the data and calculate how long it would take for the electrons to lose the energy given by the solar storm; that is, how long it would take for the third belt's influence to vanish [10].

3.1 Method

We first need to find a solar wind event by looking at the Sym-H and electron flux. Starting from the major fluctuations in the Sym-H index, if the flux is steadily decreasing, we can then select an altitude to calculate the electron decay time scale. We can choose the L to be 4 or 3.5, for example. The electron flux decays exponentially. Set the flux as z, then the decay formula is

$$z = z_0 e^{-t/\tau} \quad (1)$$

Set the altitude as y, and then we can use Eqn 1 to find the optimal y_0 and τ that can find the best sequence of t_i (time in days) and z_i (flux) value. Since we can exchange the exponential formula and the logarithmic formula, Eqn 1 is equivalent to

$$\ln(z) = \ln(z_0) - \left(\frac{t}{\tau}\right) \quad (2)$$

Then the problem becomes the standard linear regression problem, $y = kt + b$ in which we need to find the optimal $k = -1/\tau$ and $b = \ln(z_0)$. Since our data is not perfectly linear, we need to use the summation to calculate k and b. The ultimate solutions for k and b are:

$$k = \frac{n \sum y_i t_i - \sum y_i \cdot \sum t_i}{n \sum t_i^2 - (\sum t_i)^2} \quad (3)$$

$$b = \frac{\sum y_i \cdot \sum t_i^2 - \sum y_i t_i \cdot \sum t_i}{n \sum t_i^2 - (\sum t_i)^2} \quad (4)$$

3.2 1.8 MeV, L = 4

The event on March 22nd, 2015, can be a good case for 1.8 MeV and L = 4. The Figure 7 below shows how the belts are affected by the event till April 10th. In fact, this is one of the largest solar storm events in the history [10]. We can see from the graph that on March 26th, the SymH index had a very strong fluctuation, and from the 1.8 MeV energy graph, the color of the outer belt figure reflected a high particle energy. The flux index stably decreased after the storm. From these information, we know that this example could be a good case study.

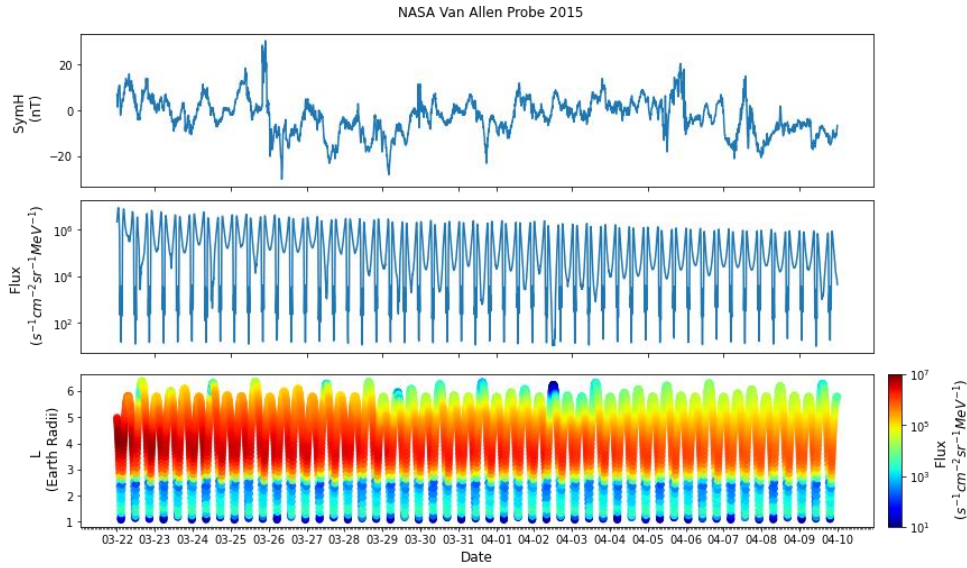


Figure 7. Solar wind event graph between March 22nd, 2015, and April 10th, 2015 at 1.8 MeV.

Through the calculations, we found that for this specific event, the decay time scale for 1.8 MeV at $L = 4$ is 8.371 days. The Figure 8 below shows the regression line of the data. As we can see, the regression line (used Equation 2 as the fitting formula) showed us the March 22nd case has a clear linear trend.

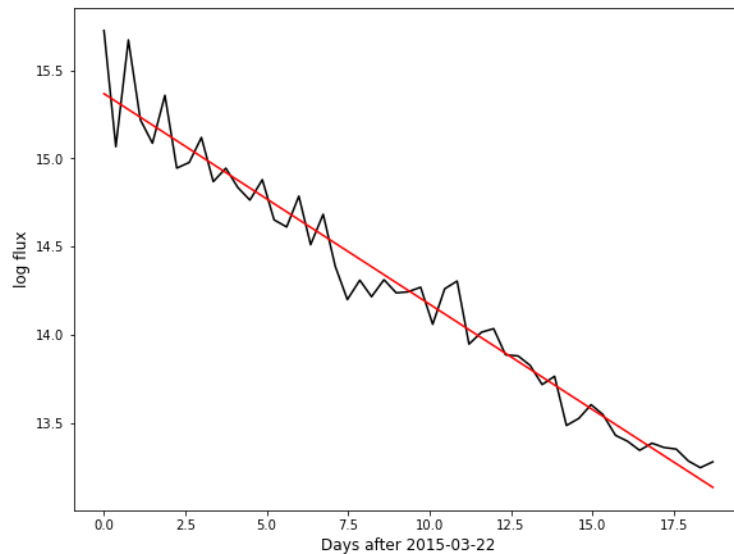


Figure 8. The fitted regression line for the first case study.

3.3 4.2 MeV, $L = 3.5$

The event on March 29th, 2013, can be a good case for 4.2 MeV and $L = 3.5$. The Figure 9 below shows how the belts are affected by the event till April 24th. We can see from the graph that on March 28th, the SymH index had a very strong fluctuation, then in April 6th and April 14th, the SymH index had strong fluctuations again which means this storm event is more complicated and hard to analyze than the March 22nd case. From the 4.2 MeV energy graph, the color of the outer belt figure reflected a high particle energy. The flux index stably decreased after the storm just like the March 22nd case.

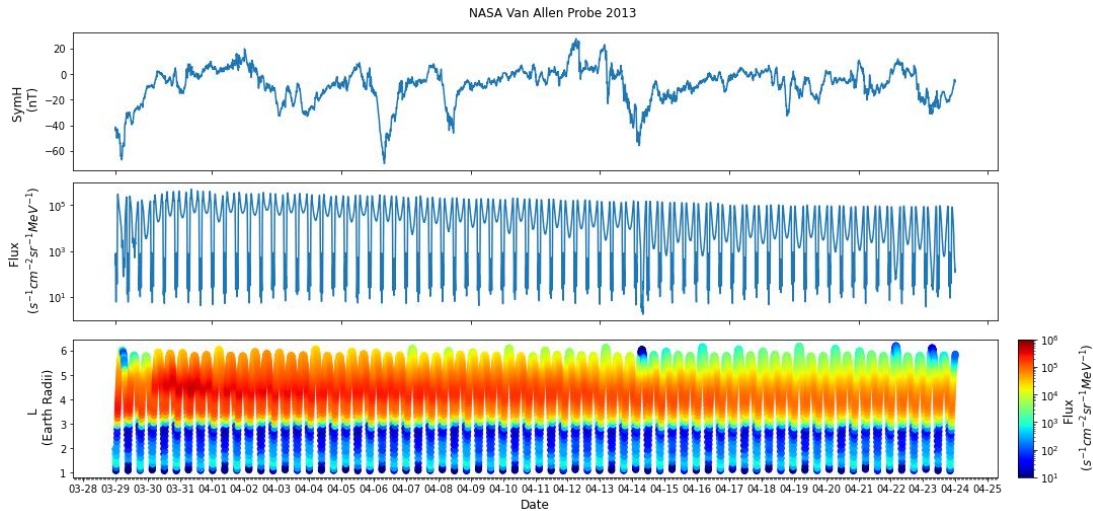


Fig 9. Solar wind event graph between March 29nd, 2015 and April 24th, 2015 at 4.2 MeV.

Through the calculations, we found that for this specific event, the decay time scale for 4.2 MeV at $L = 3.5$ is 21.716 days. The reason why the decay time scale is much bigger than the previous case may be the extended solar storm event which is much more complicated than the one shown in figure 7. The Figure 10 below shows the regression line (used equation 2 as the formula) of the data. Although the fluctuation is much stronger than the previous case, the flux still has a linear trend.

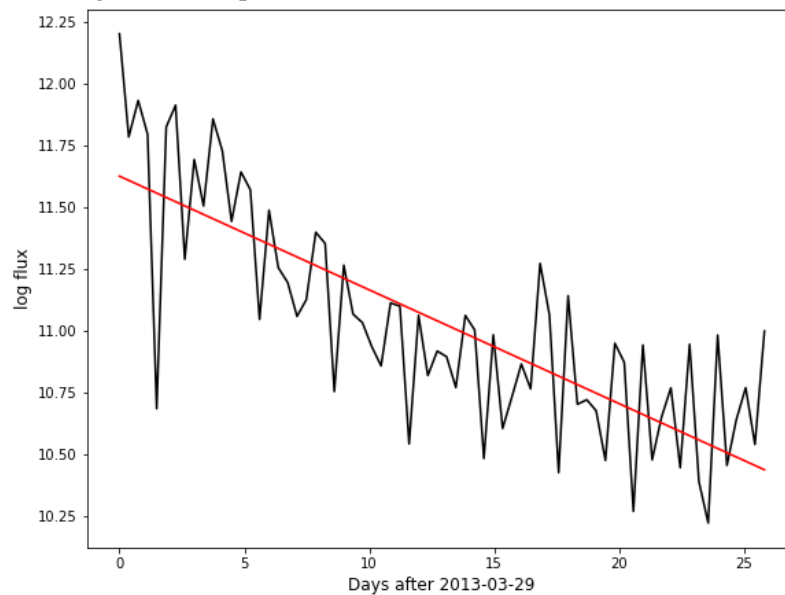


Figure 10. The fitted regression line for the second case study.

4. Conclusion

To put it in a nutshell, the dynamic of the electron flux in the radiation belt is closely associated with the Sym-H index, which reflects the solar wind effects. When the Sym-H index has a strong fluctuation, the relativistic electron flux enhances in a timescale of one day, and then steadily decay. The radiation belt generally exhibit a two-belt structure, especially at relatively low energies (e.g., 1.8 MeV), while we also observed three-belt structure, especially at energy levels above 3.4 MeV, and the remanent belt usually locates between $2.6 < L < 3.2$. We calculated the electron decay time scales in two typical cases. By analyzing the geomagnetic event from March 22nd to April 10th of 2015, we show that the 1.8 MeV

electron decay time scale at L=4 is about 8 days. By studying the geomagnetic event from March 29th to April 24th of 2013, we indicate the decay time scale of 4.2 MeV electrons at L=3.5 is about 21 days.

Reference

- [1] Pinto, V. A., Bortnik, J., Moya, P. S., Lyons, L. R., Sibeck, D. G., Kanekal, S. G., et al. (2018). Characteristics, occurrence, and decay rates of remnant belts associated with three-belt events in the Earth's radiation belts. *Geophysical Research Letters*, 45, 12,099–12,107. <https://doi.org/10.1029/2018GL080274>
- [2] Scott, K. (2020, May 19). What are the Van Allen Radiation Belts? Space Center Houston. Retrieved December 4, 2022, from <https://spacecenter.org/what-are-the-van-allen-radiation-belts/>
- [3] Radiation belts, energetic particles encircling the Earth. BIRA. (n.d.). Retrieved December 4, 2022, from <https://www.bira-iasb.be/en/encyclopedia/radiation-belts-energetic-particles-encircling-earth>
- [4] Zell, H. (2015, May 18). Van Allen Probes - Science. NASA. Retrieved December 4, 2022, from https://www.nasa.gov/mission_pages/rbsp/science/index.html
- [5] Zell, H. (2015, March 18). Van allen probes mission overview. NASA. Retrieved December 4, 2022, from https://www.nasa.gov/mission_pages/rbsp/mission/index.html
- [6] Garner, R. (2015, May 18). Van Allen probes - spacecraft and Instruments. NASA. Retrieved December 4, 2022, from https://www.nasa.gov/mission_pages/rbsp/spacecraft/index.html
- [7] Geomagnetic storms. Geomagnetic Storms | NOAA / NWS Space Weather Prediction Center. (n.d.). Retrieved December 4, 2022, from <https://www.swpc.noaa.gov/phenomena/geomagnetic-storms>
- [8] Baker, D. N., Kanekal, S. G., Hoxie, V. C., Henderson, M. G., Li, X., Spence, H. E., Elkington, S. R., Friedel, R. H., Goldstein, J., Hudson, M. K., Reeves, G. D., Thorne, R. M., Kletzing, C. A., & Claudepierre, S. G. (2013). A long-lived relativistic electron storage ring embedded in earth's outer van allen belt. *Science*, 340(6129), 186–190. <https://doi.org/10.1126/science.1233518>
- [9] Wanliss, J. A., & Showalter, K. M. (2006). High-resolution global storm index:dstversus sym-H. *Journal of Geophysical Research*, 111(A2). <https://doi.org/10.1029/2005ja011034>
- [10] Baker, D. N., et al. (2016), Highly relativistic radiation belt electron acceleration, transport, and loss: Large solar storm events of March and June 2015, *J. Geophys. Res. Space Physics*, 121, 6647–6660, doi:10.1002/2016JA022502.